Numerical upper bounds on ropelengths of large physical knots

2006 J. Phys. A: Math. Gen. 39 4829

(http://iopscience.iop.org/0305-4470/39/18/004)

INSTITUTE OF PHYSICS PUBLISHING JOURNAL OF PHYSICS A: MATHEMATICAL AND GENERAL

J. Phys. A: Math. Gen. **39** (2006) 4829–4843 doi:10.1088/0305-4470/39/18/004

Numerical upper bounds on ropelengths of large physical knots

Y Diao[1], C Ernst[2,5], V Kavuluru[3] and U Ziegler[4,6]

[1] Department of Mathematics and Statistics, University of North Carolina at Charlotte, Charlotte, NC 28223, USA
[2] Department of Mathematics, Western Kentucky University, Bowling Green, KY 42101, USA
[3] Department of Computer Science, University of Kentucky, Lexington, KY 40506, USA
[4] Department of Computer Science, Western Kentucky University, Bowling Green, KY 42101, USA

E-mail: claus.ernst@wku.edu and uta.ziegler@wku.edu

Received 31 January 2006, in final form 14 March 2006
Published 19 April 2006
Online at stacks.iop.org/JPhysA/39/4829

Abstract

Numerical computations explored for this paper show that an upper bound on the ropelength of large knots with crossing number n grows as fast as $n \ln^2 n$. The algorithms to randomly generate samples of such large knots and to determine an upper bound on the ropelength for each knot are described. The numeric results are presented and compared to the smallest known theoretical upper bounds on ropelength.

PACS numbers: 02.10.Kn, 02.40.Sf
Mathematics Subject Classification: 57M25

1. Introduction

Take a rope, weave the ends in any way you like, potentially generating an entangled mess, and then fuse the two ends together. You just generated a random 'thick knot'—as opposed to the abstract knots studied extensively in knot theory, which do not take any volume in space. New applications of knot theory in biophysics and biochemistry have focused interest on knotted molecules which are physical knots that take up some real space and have particular geometric shapes. Such knots are modelled by the so-called thick knots, which have been studied in recent years. See for example [5, 6, 8, 9, 15, 18, 27]. The *thickness* of a smooth knot can be thought of, intuitively, as the radius of the largest embedded normal tube around the knot, although slight variations of the definition do exist. A *thick knot* is a smooth knot with a positive thickness and the *ropelength* of a thick knot is the quotient of its arc length

[5] To whom correspondence regarding the theoretical aspect of the paper should be addressed.
[6] To whom correspondence regarding the computational aspect of the paper should be addressed.

(i.e. the length of the centre curve in the tube) over its thickness. This quotient ensures that the ropelength is independent of the actual thickness of the tube.

An essential problem concerning thick knots asks about the ropelength of a knot, namely the minimum length of rope (of unit thickness) required to tie the knot. This is a challenging problem. In fact, there are no analytic results which establish the (exact) minimum ropelength of any non-trivial knot. Much known theoretical and numerical work in the literature has been devoted either to the estimations of the ropelengths for relatively small knots [6, 8, 9, 22–24, 29], or to establishing various upper and lower bounds of ropelengths [2–4, 6, 9, 12, 18]. In this paper, we focus our attention on the upper bound part of the knot ropelength problem. Although some upper bounds for the ropelengths of non-trivial knots have been established [18], these are generally believed not to be optimal upper bounds. On the other hand, numerical studies on ropelengths so far are limited to relatively small knots, which cannot provide a good picture for the behaviour of knot ropelengths in general. This paper helps in gaining a better understanding of the ropelengths of non-trivial knots through numerical studies of large random knots. The authors developed and implemented algorithms which generate and embed large knots on the cubic lattice in three-dimensional space. The length of these embeddings of knots gives rise to an upper bound on the ropelength.

The next section introduces some basic terminologies needed to understand the remainder of the paper, as well as some known theoretical results and open questions regarding the knot ropelength problem. This is followed by sections which describe the algorithms used to sample large knots and how to embed the generated knots. Discussions of the methods employed, the numeric results and comparative results known from other specialized knot embedding algorithms conclude the paper.

2. Basic knot theory

In this paper, a knot K is a piecewise smooth simple closed curve in three-dimensional space. Intuitively, if one can continuously deform a knot K_1 to another knot K_2, then K_1 and K_2 are considered the same knot and are said to be of the same *knot type*. The corresponding continuous deformation is called an *ambient isotopy*. For a fixed knot K, a knot diagram of K is a projection of K onto a plane. That is, if $p : \mathbb{R}^3 \to \mathbb{R}^2$ is the projection map, then $p(K) = D \subset \mathbb{R}^2$ is the corresponding projection of K. D may not be a simple closed curve since it can contain self-intersections. D is a *regular projection* of K if the set $\{x \in D : |p^{-1}(x)| > 1\}$ is finite and the set $\{x \in D : |p^{-1}(x)| > 2\}$ is empty (here $|p^{-1}(x)|$ means the number of points in the set $p^{-1}(x)$). In other words, in the diagram D no more than two arcs of D cross at the same point in the projection and there are only finitely many such crossings. At each intersection one of the strands of the knot is below or above the other strand. For example, the right-hand side of figure 2 is a regular projection of a knot with eight crossings where the over/under strands are clearly marked. An intersection in a regular projection is called a crossing in the knot diagram and one can count the number of crossings in such a regular projection. Apparently, such a number not only depends on the knot type of K, it also depends on the geometrical shape of K and the projection direction chosen. The minimum number of crossings in all regular projections of all knots having the same knot type as K is called the *crossing number* of the knot K and is denoted by $Cr(K)$. Of course, by this definition, if K_1 and K_2 are of the same knot type, then we have $Cr(K_1) = Cr(K_2)$. Furthermore, it may be the case that for a knot K' having the same knot type with K, none of the regular projections of K' has the crossing number $Cr(K)$. A diagram D of a knot K is *minimal* if the number of crossings in the diagram equals $Cr(K)$. In this case we also say that D is a *minimum projection diagram*. On the other hand, a diagram D of a knot K is said to be a *reduced*

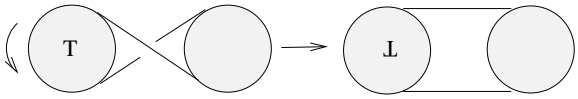

Figure 1. A knot diagram that can be reduced by a single twist.

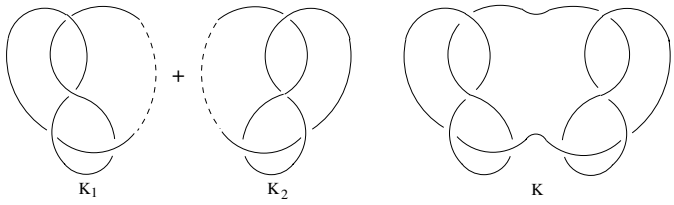

Figure 2. A composite knot $K = K_1 \# K_2$.

diagram if D does not contain a crossing that can be removed by a simple twist as shown in figure 1. Note that a reduced diagram is not necessarily a minimal projection diagram. A knot is *alternating* if there is a knot projection in which one encounters over-passes and under-passes alternatingly when travelling along the knot projection. The crossing number of an alternating knot can be determined by the fact that any alternating reduced diagram of an alternating knot is minimal, for example the diagrams K_1 and K_2 on the left-hand side of figure 2 are minimal since they are alternating and reduced. (The knot diagram on the right-hand side of figure 2 is not alternating, but it can be actually deformed to a reduced alternating diagram with the same number of crossings in it, so it is also minimal.)

A knot K is called a *composite knot* if it can be obtained by cutting open two non-trivial knots K_1 and K_2 and reconnecting the strings as shown in figure 2. We write $K = K_1 \# K_2$ and call K_1 and K_2 the *connected sum components*. Note that a knot can have more than two connected sum components. A knot K that is not a composite knot is called a *prime knot*. When a knot diagram is viewed as a 4-regular planar graph, we will call it a *prime diagram* if it is at least three-edge connected (meaning removing any two edges from the graph will not make the graph disconnected). (Actually any 4-regular graph that is three-edge connected is also four-edge connected.)

Traditionally, non-trivial knots are tabulated according to their crossing numbers. The crossing number of a knot is a fairly reliable indicator of how complex the knot is. That is, it is usually the case that the larger the crossing number, the more complicated the knot is (in terms of other knot complexity measures). In this paper, 'large knot' means a knot with a large crossing number. Similarly, a 'small knot' in this paper means a knot with a small crossing number. The tabulations of small knots can be found in most knot theory textbooks. See for example [1]. The following theorem summarizes the best known results regarding the lower and upper bounds of knot ropelengths (in terms of the power of $Cr(K)$).

Theorem 1. *There exist constants $c_1, c_2 > 0$ such that for any knot K with minimal crossing number $Cr(K)$, we have*

$$c_1 \cdot (Cr(K))^{3/4} \leqslant L(K) \leqslant c_2 \cdot (Cr(K))^{3/2}.$$

The $3/4$ power for the lower bound is sharp [12], and it was shown [13, 17] that for any p with $3/4 \leqslant p \leqslant 1$ there exist families of infinitely many knots (some of these are not prime

but are composite knots) such that $c_0 \cdot (Cr(K))^p \leqslant L(K) \leqslant c_1 \cdot (Cr(K))^p$ for some constants $c_0, c_1 > 0$ and any knot K in such a family. Thus a universal upper bound for $L(K)$ would be at least of the order of $Cr(K)$.

A common approach to answer ropelength questions about knots is to construct polygonal knots on the cubic lattice. The *cubic lattice* is the infinite graph in $\mathbf{R}^3$ whose vertices are points with integer coordinates and whose edges are unit length line segments connecting these points. Hence, there are three types of edges in the cubic lattice: those parallel to the x-axis, those parallel to the y-axis and those parallel to the z-axis. The *length* of a lattice knot F, denoted by $L(F)$, is the total number of lattice edges in F. It is well known that any polygonal knot of length n on the cubic lattice can be isotoped into a smooth knot of ropelength at most $2n$. On the other hand, it is known that for any knot K of unit thickness with ropelength $L(K)$, there is a lattice polygon P that is isotopic to K with length at most $12L(K)$ [16]. Thus, the difference in behaviour of the length of lattice knots and the ropelength of smooth knots is bounded by a constant multiplicative factor on the length. So questions and results about the length of lattice knots can be immediately rephrased as questions and results about the ropelength of knots. Conversely results about the ropelength of smooth knots translate to results about the length of lattice knots.

The upper bound in theorem 1 is achieved by an algorithm that takes a given knot and constructs a lattice embedding of the knot. The length of this lattice embedding is bounded above by the $c_2 \cdot (Cr(K))^{3/2}$ term. However, the constant used in this construction is large and the power $3/2$ is based on a worst case analysis (see [18]) that seems to be avoided in the random sample of knots shown here by a simple trick. The details of this algorithm will be discussed in section 4.

3. Random sampling of large knots

One problem in establishing the relationship between the ropelength and the crossing number of a knot is the difficulty in determining the crossing numbers for most large knots. In fact only a few special knot families have known crossing numbers (such as alternating knots, torus knots and Montesinos knots). The crossing numbers of most knots can only be determined if one exhaustively classifies all knot projections with smaller crossing numbers than the given one. This has only been done for knots up to 16 crossings [25]. Since this paper addresses knots with large crossing numbers (up to a few thousands), this exhaustive process cannot be used. It can be easily shown that any torus knot of crossing number n has ropelength at most $O(n)$. Furthermore, the ropelength of any Montesinos knot of crossing number n is also bounded above by $O(n)$ [14]. Thus, there is no need for us to study the ropelength problem for the two knot families of torus and Montesinos knots. Our sampling will be limited to prime alternating knots since we need to determine the crossing number of the knots generated. (In the last section we will point out that sampling alternating knots is enough to bound the ropelength of the non-alternating prime knots as well.)

It needs to be pointed out that it is not practical (if not impossible) to generate large prime knots by generating random polygons (closed random walks) in three-dimensional space. The reasons that random polygons will not work are the following: first, the polygon will have to be very long in order to generate complex knots. Secondly, a long random polygon tends to be composite (with many connected sum components) [10, 20, 30, 31] and, lastly, the polygon will represent a non-alternating knot whose crossing number cannot be determined even with the most powerful computer in a time efficient manner. Instead, the random sampling procedure used in this paper takes a very different approach that is based on the fact that every knot K has a regular projection that can be viewed as a 4-regular planar graph G if the crossings

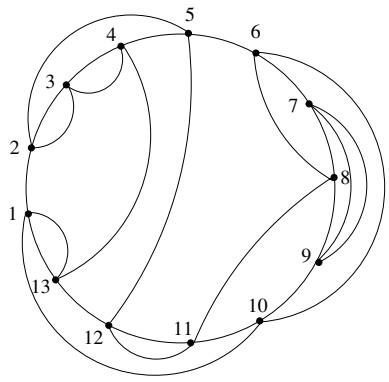

Figure 3. A small prime knot projection with 13 crossings. The Hamilton cycle is the circle and the vertices are numbered along the cycle. No 'over' and 'under' are indicated at the crossings.

are regarded as vertices and the simple curves joining the crossings are regarded as edges. Thus the authors concentrate on generating random 4-regular planar graphs G of a particular type: graphs with a Hamilton cycle. A *cycle* C of length k, where $k \geqslant 2$, is a graph which is isomorphic to the graph with vertex set $\{v_1, v_2, \ldots, v_k\}$ (all the vertices v_i are distinct) and edge set $\{v_i v_{i+1} : i = 1, \ldots, k-1\} \cup \{v_k v_1\}$. A *Hamilton cycle* in a graph G is a cycle for which the vertex set $\{v_1, v_2, \ldots, v_k\}$ equals the vertex set of the whole graph. A graph with a Hamilton cycle is said to be *Hamiltonian*. The key to the embedding algorithm described in the next section is the use of a Hamilton cycle in the graph obtained from a regular projection of the knot K. For every knot K there exists a Hamiltonian planar graph G [18] obtained from a projection of K with at most $4Cr(K)$ vertices. Figure 3 shows an example of a knot projection with a Hamilton cycle. (We need to point out that not every minimum knot projection is Hamiltonian, see [18].)

Below is a brief description of the construction of a random 4-regular planar Hamiltonian graph G that serves as a regular projection (not necessarily minimal) of the random knot to be generated, for more details see [19]. Since the problem of finding a Hamilton cycle in a large graph is computationally very difficult the construction starts with a fixed Hamilton cycle C of n vertices and develops the graph around this cycle. The n vertices will be the crossing points of the projection of the knot. Next, n edges are added to the cycle C in a random manner to create a 4-regular graph. (Pairs of vertices simply chosen at random and the two vertices in a pair are connected by an edge either entirely in the outside or entirely in the inside of the cycle C.) The graph so created is non-planar with a probability of almost 1. (Actually, the average number of intersections between the n new edges is of the order of $O(n^2)$.) The resulting non-planar graph is modified into a 4-regular planar graph by removing the intersections between the n new edges one intersection at a time as shown in figure 4 (left). An edge is picked at random and the first intersection with another edge is identified. Then the two edges are broken at the crossing and recombined into two new edges that no longer cross each other. There are two possibilities and one is chosen at random.

The 4-regular graph obtained at the end of this process is usually a projection diagram of a link with more than one component. To combine the components randomly, a vertex v in the graph is picked at random. The faces containing v are processed in a random order. For each face, the algorithm identifies the non-Hamilton edge on this face with endpoint v and the component to which it belongs. It then searches through the edges of the face, looking

Figure 4. Left: the two possibilities of removing an unwanted crossing by replacing the crossings of two edges with two non-crossing edges. Right: two edges of different components are recombined to form one component.

for an edge that is not on the Hamilton cycle and which belongs to a different component. Once the algorithm finds such edges, an edge replacement move is carried out as shown on the right-hand side of figure 4. (We break the two edges at two points and recombine the ends to form two new edges. This reduces the number of components by 1.) Once a replacement move is carried out a new vertex v is picked at random and a new edge replacement move is carried out. This continues until there is only one component left. The graph obtained at this point is the graph of a knot projection and has exactly n crossings, but it is not necessarily the projection of a prime knot. To obtain projections of prime knots, the 4-regular planar graph obtained up to this point is then split into four-edge connected components based on characteristics discussed by Dowker and Thistlethwaite [21]. A component G obtained at the end of this process is a regular projection of some prime knot, depending on how the over/under passes are assigned at each vertex. Assigning the over/under passes at the vertices so that an alternating knot is obtained, results in an alternating prime knot whose crossing number is exactly the number of vertices in G. The knot projection shown in figure 3 is a typical example generated by the algorithm.

Remark 1. The reasons that we are only interested in prime knot diagrams are as follows: researchers in knot theory traditionally concentrate their efforts on prime knots with the understanding that the behaviour of composite knots can be explained once we understand the behaviour of prime knots. In the case of ropelength for a composite knot K, say $K = K_1\#K_2\#\cdots\#K_p$, where $K_1, K_2, \ldots, K_p$ are prime knots, the ropelength of K is easily shown to be bounded by the sum of the ropelengths of K_j's. Although it is still an open question whether the crossing number of K is the sum of the crossing numbers of K_j's, it is conjectured to be true. In this sense the upper bounds of ropelengths of prime knots will give rise to the upper bounds of the ropelengths of composite knots.

Remark 2. When we split the knot diagram into prime knot diagrams, the control over the number of crossings in the final prime knot is lost. In other words, we start with a graph with n vertices and we obtain at the end graphs that are projections of prime knots of varying sizes; see section 5 for some data on the size of the prime knots obtained.

Remark 3. For any given knot type $\mathcal{K}$ with crossing number m, there exists a knot K (as a closed curve in 3-space) with knot type $\mathcal{K}$ such that the graph G of a regular projection D of K can be generated by the above process (though this graph may not represent a minimal projection of $\mathcal{K}$). Furthermore, the number of crossings in D is at most $4m$. This means that our generating method is ergodic, that is, projection diagrams of all prime knots can be generated by this method.

Remark 4. At this stage, not much can be said about the probability distribution of the knots generated by the above algorithm since the space of the large knots is not well understood. Because the algorithm generates prime knot diagrams based on Hamilton cycles, those prime knot diagrams with many different Hamilton cycles will have a higher probability to be

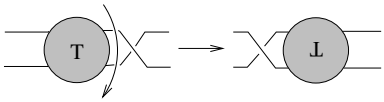

Figure 5. A single flype. T denotes a part of the diagram that is rotated by 180° by the flype.

generated than prime knot diagrams with few Hamilton cycles. The difference between the number of Hamilton cycles in two different diagrams (with the same number of crossings) can be very large even for a small number of crossings. For example, the number of Hamilton cycles for knots with 9 crossings varies from 512 for 9_1 to zero for 9_{35}. (9_{35} is the only 9-crossing alternating knot which does not have a minimum Hamiltonian projection graph.) Even if the above algorithm could generate 4-regular planar Hamiltonian graphs with n vertices with uniform probability this still would not generate knots (with the same crossing number n) with uniform probability. For example, in the case of alternating knots, any two minimum projection diagrams D and D' of the same alternating knot K are flype equivalent, that is, there is a finite sequence of flypes that changes D to D' [28] (see figure 5). However a flype usually changes the underlying 4-regular graphs to a non-isomorphic graph. Thus knots having a large number of flype equivalent diagrams are more likely to appear than knots having a small number of flype equivalent diagrams.

Remark 5. Using the above algorithm the computing time to generate many large prime knot diagrams is considerable. On a standard desktop PC (Pentium 4) the average time to generate a single prime knot diagram with about 2100 to 2200 crossings was about 17 min when starting with a 3000 vertex Hamilton cycle. For a prime knot diagram with 4500 to 5000 crossings it took more than 84 min when starting with a 7000 vertex Hamilton cycle. Currently the authors are working to improve the algorithm so that larger knots can be generated within less time.

4. Deriving upper bounds for ropelengths of large knots

For any given knot K (or rather, the graph G of a regular projection of K), our algorithm will construct a polygonal knot on the cubic lattice that has the same knot type as K, while trying to keep the length of the polygon small. The length of this polygonal knot then gives rise to an upper bound on the ropelength of the knot. Recall that the length of the lattice knot F, denoted by $L(F)$, is the total number of lattice edges in F. The key in the construction of the lattice knot F is the Hamilton cycle C in G. Let $n = |V(G)|$ be the number of vertices in G. Let $v_1, \ldots, v_n$ denote the vertices of G which occur on C in the cyclic order listed. Let $k = \lceil \sqrt{n} \rceil$. Observe that as a simple closed curve in the plane $z = 0$, C divides the plane $z = 0$ into two closed regions, one bounded and one unbounded. The non-Hamilton edges of G are then divided into two groups: those in the bounded region, called *B-edges*, and those in the unbounded region, called *U-edges*. In figure 3, edges 1–10, 2–5 and 11–12 are examples of U-edges and edges 1–13, 5–12 and 6–8 are examples of B-edges. Since G is 4-regular with n vertices, it has $2n$ edges, of which n form the Hamilton cycle C and the other n are the U- and B-edges.

The algorithm will first embed the Hamilton cycle C into the box $[0, 3k] \times [0, 3k] \times [-1, 1]$ in $O(n)$ steps in the form of a comb with $\lceil k/2 \rceil$ teeth and $k \approx \sqrt{(n)}$. All teeth, except possibly the last one, have length $O(k)$. Figure 6 shows the cases for $n = 14$ and $n = 23$.

Next the U-edges are embedded in the half-space $z \geqslant 1$ and, finally, the B-edges in a similar way into the half-space $z \leqslant -1$. The embedding of the U-edges and B-edges has to

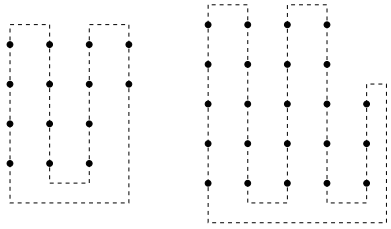

Figure 6. A planar Hamiltonian projection forming a comb with 14 or 23 vertices.

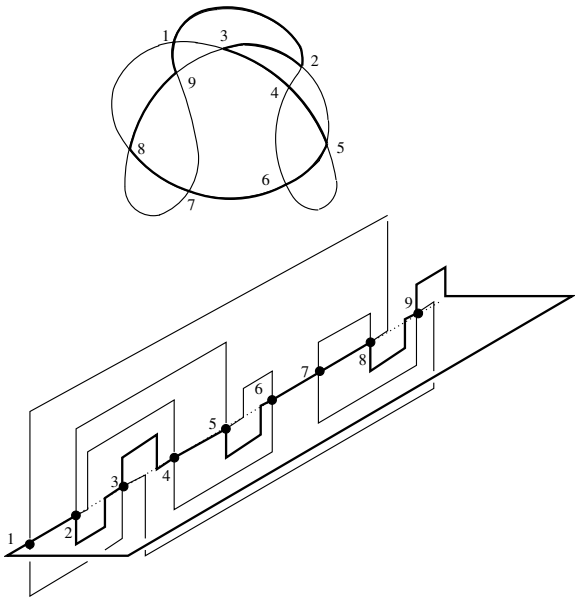

Figure 7. A Hamiltonian projection of the 9-crossing knot 9_{32} and its realization in the cubic lattice.

be done very carefully in order to preserve the knot type of K. It is shown in [18] that each of the n U- and B-edges can be embedded into the lattice using a lattice path of length at most $O(\sqrt{n})$; hence K can be embedded into the cubic lattice with a length at most $O(n^{3/2})$. In other words, $O(n^{3/2})$ is a universal upper bound for the ropelength of any knot with crossing number n. Figure 7 shows the lattice embedding of a 4-regular graph (not the knot) in the case that the vertices are lined up along a line segment on the Hamilton cycle. This is done so that the embeddings of the edges not on the Hamilton cycle can be visualized easily by the reader.

The left-hand side of figure 8 shows the actual embedding of a 22-crossing knot generated by the algorithm described in the last section. The Hamilton cycle now follows the comb shape described in figure 6 and is no longer easily visible. Figure 9 shows the embedding of a 415-crossing knot with a length of 7528. Here it is almost impossible to follow the path of the knot embedding.

The upper bound $O(n^{3/2})$ obtained in [18] arises from the fact that in the worst case each of the n U- and B-edges in $G\backslash C$ requires a length of $O(\sqrt{n})$ in its embedding on the cubic lattice. However, it is quite possible that in most cases this worst case scenario does not happen and the $O(n^{3/2})$ bound can be improved. Each B-edge is associated with a recursively defined

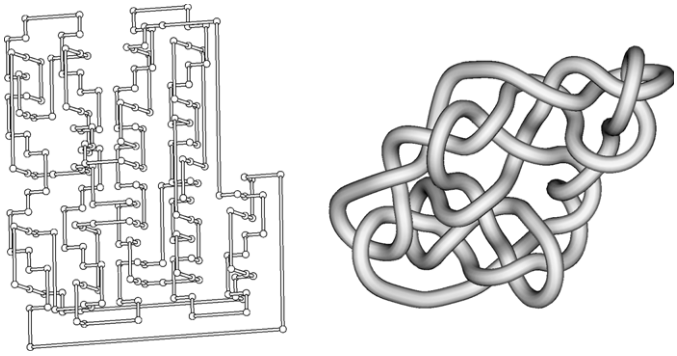

Figure 8. On the left is a lattice embedding of a 22-crossing knot generated by the generating algorithm discussed in section 3. On the right is a smooth embedding of the same knot created by a ropelength minimizing software designed for smooth and small knots.

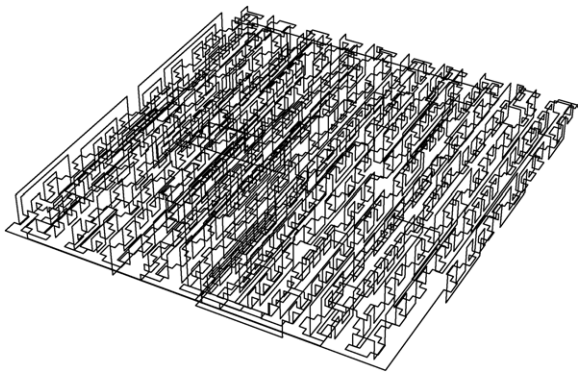

Figure 9. A lattice embedding of a knot with 415 crossings with a length of 7528 steps.

number, called the *level* of that edge. The level of a B-edge e (starting at vertex k and ending at vertex p, with $k \leqslant p$) is one more than the highest level number of any B-edge 'captured' between e and the Hamilton cycle between vertices k and p. A B-edge is 'captured' if it starts and ends between k and p. If there is no B-edge captured between e and the Hamilton cycle at all, then e has level number 1. The level numbers for the U-edges are defined in a similar manner. For example, the U-edge from vertex 1 to vertex 8 in figure 7 is a level 3 edge since it captures the level 2 edge from vertex 2 to vertex 5. In our embedding algorithm, the level number of an edge e determines how far away from the plane $z = 0$ the lattice path that is the embedding of e will move. Thus the key to finding a good upper bound on the ropelength of a knot by our algorithm is to find a diagram of the knot that contains a Hamilton cycle C resulting in low level numbers for the edges not in the cycle C. The level numbers of the edges not on the Hamilton cycle C depend on the vertex on the Hamilton cycle chosen as a starting vertex when the Hamilton cycle is embedded in the comb shape in the plane $z = 0$. The embedding length data reported in the next section are the minimum ropelength found when allowing each vertex on the Hamilton cycle C to be the starting vertex on the comb-shaped Hamilton cycle embedding. That is each ropelength reported is the minimum obtained from n different embeddings of the knot. This trick leads to a significant shortening of ropelength reported in the next section.

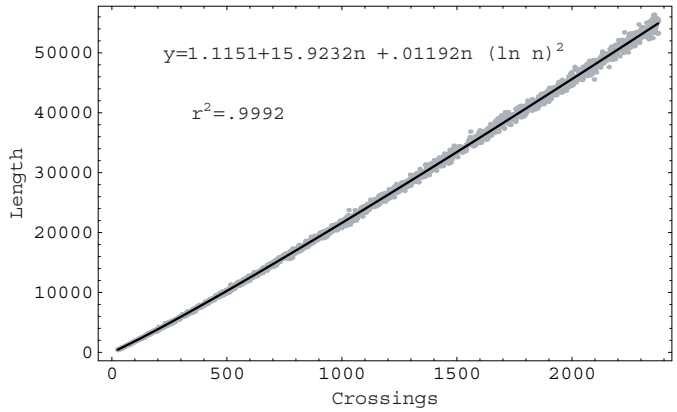

Figure 10. The evenly spread sample of 2350 knots together with the best $a + bn + cn \ln^2 n$ fit curve, which is $y = 1.1151 + 15.9232n + 0.1192n \ln^2 n$ with $r^2 = 0.9992$. The x-axis is the crossing number of the knot and the y-axis shows the length of the cubic lattice embedding.

5. Numerical results

The algorithm described in section 3 produces random samples of prime knot diagrams that are heavily weighted towards small knot diagrams. This happens since we have to cut the diagrams apart into prime knot diagrams. For example, if one starts with $n = 500$ (or $n = 3000$) vertices in the initial Hamilton cycle, then one obtains knot diagrams with $n = 500$ (or $n = 3000$) crossings. However these are not prime knot diagrams. After cutting these knot diagrams into prime knot diagrams only about 8.2 (for $n = 500$) or 4.0 (for $n = 3000$) per cent of them have more than 30 crossings. (These percentages are based on samples of 10 000 elements, see [19] for details.) In order to generate a sample of knot diagrams that are evenly spread, enough prime knot diagrams were generated so that it was possible to pick randomly ten prime knot diagrams out of any interval ranging over ten consecutive crossing numbers. To be more precise, the sample contains 2350 knots with ten knot diagrams in each of the intervals 25–34, 35–44, 45–54, . . . , 2365–2374, picked at random out of the generated prime knot diagrams. For the sake of simplicity in stating the numerical results, the over/under passes at the crossings were assigned so that the resulting knots are alternating. Thus the number of crossings in a diagram equals the minimum crossing number of the knot. The implication of the numerical results for non-alternating knots is discussed in the next section. Each of these 2350 knots was embedded into the cubic lattice as described in section 4.

Figure 10 shows the length data produced by the algorithm. It can be seen that the growth of the length is slightly more than linear. The data were fit with the model $y = a + bn + cn \ln^2 n$ (where y is the ropelength upper bound and n is the crossing number of the knots) due to the following considerations. First, based on the discussion following theorem 1 it is known that an overall upper bound on the ropelength is at least linear in terms of the crossing number, so the fit function used needs to be at least linear (although researchers have yet to produce any example of knot families whose ropelengths grow faster than linear in terms of their crossing numbers). Second, it has been shown that a planar 4-regular graph of n vertices (which is equivalent to a regular projection of a knot with n crossings) is isomorphic to a graph embedded in the cubic lattice with a total length at most of the order of $O(n \ln^2 n)$ [26] and there are examples showing that this cannot be further improved in general. Since a graph isomorphism does not have to keep the topology of original planar graph, it is much less restrictive than

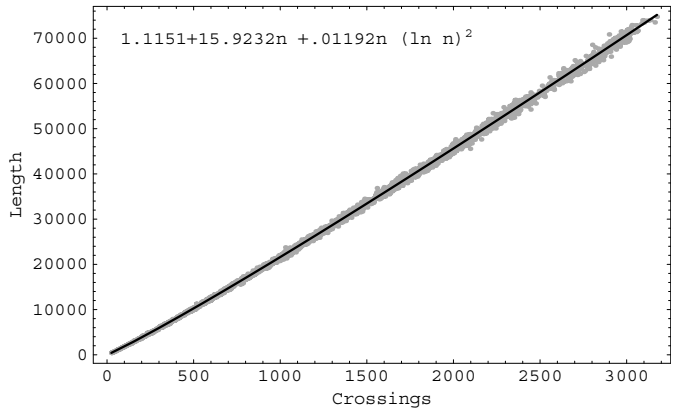

Figure 11. The length data of 2790 knots with crossing numbers ranging from 25 to 3174 together with the plot of the function $y = 1.1151 + 15.9232n + 0.1192n \ln^2 n$.

a knot embedding. (For example a graph isomorphism does not have to preserve the cyclic order of edges around a vertex, while this cyclic order must be preserved if one wants to keep the knot type unchanged.) It is thus reasonable to conjecture that a general ropelength upper bound is at least of the order of $O(n \ln^2 n)$ for knots with crossing number n. Figure 10 shows that the chosen model fits the data nearly perfectly.

To test whether the fit $y = 1.1151 + 15.9232n + 0.1192n \ln^2 n$ works well for knots with larger crossing numbers, it was plotted against the length data of 440 additional knots that were generated in addition to the smaller knots already used in the sample above. These larger knots have crossing numbers ranging from 2375 to 3174. The combined sample is shown in figure 11. It can be clearly seen that $y = 1.1151 + 15.9232n + 0.1192n \ln^2 n$ still fits very well for the ropelengths of the extended sample.

To check how representative our collected sample is, we generated and collected 1601 400-crossing prime knots, 1092 800-crossing prime knots and 1446 1000-crossing prime knots. Figure 12 shows a bar graph of the ropelength distributions of these knots. In each of the bar graphs the ropelength distribution is approximately normal.

Figure 13 shows the length data of figure 10 for 400 to 1000 crossings together with the knots in the sample of figure 12. The small vertical lines indicate the minimal and maximal embedding lengths observed in the samples with 400, 800 and 1000 crossings. The black point on the vertical lines indicates the average embedding length of the three samples at 400, 800 and 1000 crossings. It is evident that the sample density in the original sample in figure 10 is representative since the much larger sample sizes at 400, 800 and 1000 crossings did not significantly change the outcome.

6. Discussions

The algorithm that generates the lattice embeddings has the advantage that it can handle very large knots with thousands, or even tens of thousands of crossings. The ropelength upper bounds produced by the lattice embedding computations indicate that the ropelengths of most knots are bounded above by $O(n \ln^2 n)$. The embedding algorithm used here is tailored to generate lattice embeddings for very large knots. The ropelength upper bounds derived are only meaningful for large knots since the use of the Hamilton cycle inevitably causes

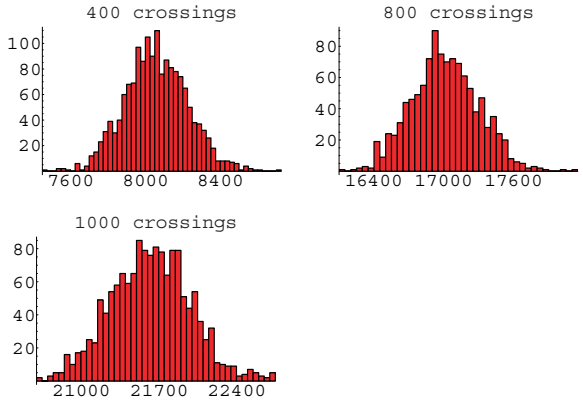

Figure 12. The embedding length distributions of the 1601 400-crossing prime knots, 1092 800-crossing prime knots and 1446 1000-crossing prime knots. The x-axis shows the embedding length and the y-axis shows the frequency of occurrences.

(This figure is in colour only in the electronic version)

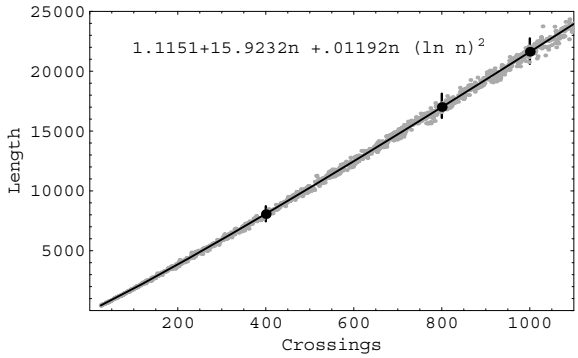

Figure 13. Embedding length data from figure 10 for 25 to 1000 crossings together with the length data of the samples at 400, 800 and 1000 crossings. The small vertical lines show the spread in the embedding lengths of the knots of the samples.

significant length inefficiencies in the embedding of small knots. However, even though the embedding lengths derived here are not optimal, they are still much shorter than the best (theoretically proven) ropelength upper bounds currently available. For knots with crossing numbers in the range up to 470 crossings, the best known theoretical ropelength upper bound is given by $y = 1.64n^2 + 7.69n + 6.74$ (where n is the crossing number of the knot) [4]. Knot embedding on the cubic lattice has a thickness of $1/2$. To compare this with knot embedding of thickness 1 we need to multiply the length of the lattice embedding by 2. Comparing the above upper bound with twice the best fit function $y = 2(1.1151 + 15.9232n + 0.1192n \ln^2 n)$ derived from the presented data, we find that for knots starting with 16 crossings twice the best fit function is already smaller. For the knots with more than 470 crossings and Hamiltonian minimum projections the best known upper bound is an $n^{3/2}$-power function $y = 34n^{3/2} + 42n + 22\sqrt{(n)} + 22$ [18], see theorem 1 and figure 14. This strongly suggests that there is still much room for improvement to the known results about the theoretical ropelength upper bounds.

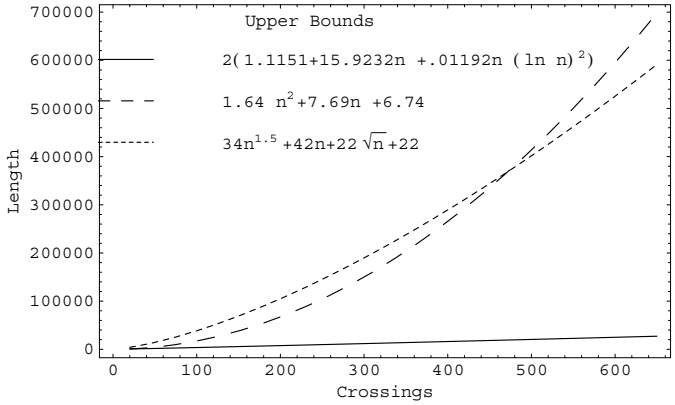

Figure 14. The comparison of the best fit function $y = 2(1.1151 + 15.9232n + 0.1192n\ln^2 n)$ with the best known upper bound functions $y = 1.64n^2 + 7.69n + 6.74$ and $y = 34n^{3/2} + 42n + 22\sqrt{(n)} + 22$.

Although there are algorithms designed to approximate the actual ropelength of a knot (usually through controlling the gradient flow), they only work well for small knots (with less than 50 crossings) and cannot handle the large knots discussed here. These algorithms have mostly been used to approximate the ropelength of a given knot in the current knot tables (such a knot would only have crossing number up to 16). Figure 8 is an example of a 22-crossing knot shown with two configurations: one embedded in the lattice by our algorithm and the other (smooth) one close to a ropelength minimizer of the knot computed by a program called 'ridgerunner' due to Rawdon/Piatek (see [7] for their related work). The 'smooth' embedding uses 233 points to describe its core curve and the approximated ropelength is around 198.5. On the other hand, the lattice embedding has a length of 364. Since the lattice embedding converts to a smooth embedding with a thickness of $1/2$, the ropelength bound given by the lattice embedding is slightly smaller than 728, which is less than four times the actual ropelength. We have compared several other small examples and in all cases the ropelength upper bounds given by the lattice embedding are smaller than four times the actual ropelengths. It is understandable that the algorithms designed to search for the ropelength minimizers of knots will provide much better ropelength upper bounds than our embedding algorithm, since the aim of the embedding algorithm is to find a reasonable upper bound of the ropelength for a large knot in a timely manner.

In figure 15, the ratios between the lengths of the embedded knots (from the sample) and the volumes of the smallest rectangular boxes containing these embeddings are shown. The ratio tells us the percentage of the lattice vertices within the box occupied by the embedding. It seems that this percentage stabilizes around 15%. This may be viewed as a measure of how much improvement might be possible by using the available space more efficiently.

Finally, we need to point out that our data also support an $O(n\ln^2 n)$ growth as an upper bound on ropelength for non-alternating knots. The length of the lattice embedding generated by our algorithm depends almost exclusively on the underlying graph. It remains almost unchanged when the over- and under-information at the vertices of the graph is changed in different ways to generate non-alternating knot diagrams. Thus the best fit function $y = 1.1151 + 15.9232n + 0.1192n\ln^2 n$ works when viewed in the context of a sample of Hamiltonian knot diagrams of n crossings that includes alternating and non-alternating knots. Such a knot diagram may not be minimal; however, we do know that any knot K (alternating and non-alternating) will admit a Hamiltonian diagram with at most $4Cr(K)$ crossings. Thus

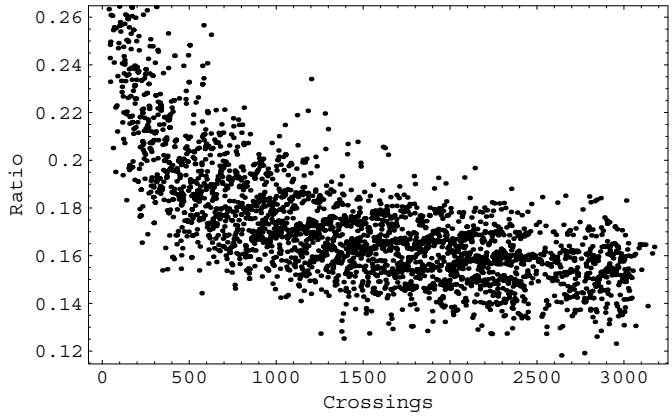

Figure 15. The ratio of embedding length divided by the volume of a box containing the embedding.

in the worst case a non-alternating knot with crossing number n behaves like a knot with $4n$ crossings in our sample.

Acknowledgments

The authors wish to thank M Piatek and E Rawdon for providing the numeric ropelength data for the smooth knot ropelength example in this paper. The authors are currently supported in part by NSF Grant DMS-0310562.

References

[1] Adams C 1994 *The Knot Book* (New York: Freeman)
[2] Buck G 1998 *Nature* **392** 238–9
[3] Buck G and Simon J 1999 *Topol. Appl.* **91** 245–57
[4] Cantarella J, Faber X W and Mullikin C A 2003 *Topol. Appl.* **135** 253–64
[5] Cantarella J, Kusner R B and Sullivan J M 1998 *Nature* **392** 237–8
[6] Cantarella J, Kusner R B and Sullivan J M 2002 *Inventiones Mathematicae* **150** 257–86
[7] Cantarella J, Piatek M and Rawdon E 2005 *Proc. 16th IEEE Visualization 2005* vol 150 pp 575–82
[8] Delle E, Diao Y and Sullivan J M 2006 *Geom. Topol.*, at press
[9] Diao Y 2003 *J. Knot Theory Ramif.* **12** 1–16
[10] Diao Y 1995 *J. Knot Theory Ramif.* **4** 189–96
[11] Diao Y 1993 *J. Knot Theory Ramif.* **2** 413–25
[12] Diao Y and Ernst C 1998 *Topol. Appl.* **90** 1–9
[13] Diao Y and Ernst C 2004 *JP J. Geom. Topol.* **4** 197–208
[14] Diao Y and Ernst C 2006 *J. Knot Theory Ramif.* at press
[15] Diao Y, Ernst C and Janse Van Rensburg E J 1999 *Math. Proc. Camb. Phil. Soc.* **126** 293–310
[16] Diao Y, Ernst C and Janse Van Rensburg E J 2002 *J. Knot Theory Ramif.* **11** 199–210
[17] Diao Y, Ernst C and Thistlethwaite M 2003 *J. Knot Theory Ramif.* **12** 709–15
[18] Diao Y, Ernst C and Yu X 2004 *Topol. Appl.* **136** 7–36
[19] Diao Y, Ernst C and Ziegler U 2005 *Physical and Numerical Models in Knot Theory* ed J A Calvo, K C Millett, E J Rawdon and A Stasiak (*Series on Knots and Everything* vol 36) (Singapore: World Scientific) pp 473–94
[20] Diao Y, Pippenger N and Sumners D W 1994 *J. Knot Theory Ramif.* **3** 419–29
[21] Dowker C H and Thistlethwaite M 1983 *Topol. Appl.* **16** 19–31
[22] Gonzalez O and R de la Llave 2003 *J. Knot Theory Ramif.* **12** 123–33
[23] Gonzalez O and Maddocks J H 1999 *Proc. Natl Acad. Sci. (USA)* **96** 4769–73
[24] Gonzalez O, Maddocks J H, Schuricht F and von der Mosel H 2002 *Calc. Var. Partial Differ. Equ.* **14** 29–68
[25] Hoste J, Thistlethwaite M and Weeks J 1998 *Math. Intelligencer* **20** 33–48

[26] Leiserson C E 1980 *Proc. 21st Ann. IEEE Symp. on Foundations of Computer Science* pp 270–81
[27] Litherland R, Simon J, Durumeric O and Rawdon E 1999 *Topol. Appl.* **91** 233–44
[28] Menasco W and Thistlethwaite M 1991 *Bull. Am. Soc.* **25** 404–12
[29] Pieranski P 1998 *Ideal Knots* ed A Stasiak, V Katritch and L H Kauffman (Singapore: World Scientific) pp 20–41
[30] Pippenger N 1989 *Discrete Appl. Math.* **25** 273
[31] Sumners D W and Whittington S G 1988 *J. Phys. A: Math. Gen.* **21** 1689–94